Difference-frequency generation in AlGaAs Bragg reflection waveguides

Jun-Bo Han, Payam Abolghasem, Dongpeng Kang, Bhavin J. Bijlani, and Amr S. Helmy*

The Edward S. Rogers Sr. Department of Electrical and Computer Engineering, University of Toronto, 10 King's College Road, Toronto, Ontario M5S 3G4, Canada

**Corresponding author: a.helmy@utoronto.ca*

Received May 4, 2010; revised June 11, 2010; accepted June 12, 2010; posted June 18, 2010 (Doc. ID 127862); published July 2, 2010

We demonstrate Type II difference-frequency generation (DFG) around 1550 nm in AlGaAs Bragg reflection waveguides using a pump around 778 nm and a signal within the C-band range. Difference-frequency power of 0.95 nW was obtained using a pump power of 62.9 mW and a signal power of 2.9 mW. Nonlinear conversion efficiency was estimated to be $2.5 \times 10^{-2}\%/\mathrm{W}^{-1}\ \mathrm{cm}^{-2}$ in a 1.5-mm-long sample. Using numerical simulations, the phase-matching bandwidth was predicted to be 100 nm, while the measured DFG showed no sign of bandwidth limitation across a wavelength span of 40 nm, which was limited by instrumentation.

OCIS codes: 190.4410, 160.4330, 130.3120, 230.1480, 190.2620.

Tunable coherent infrared sources are indispensible for a vast number of optical applications, including infrared spectroscopy, environmental monitoring, chemical sensing, medical diagnostics, and terahertz generation. Difference-frequency generation (DFG) is an attractive technique for the generation of widely tunable coherent infrared radiation, where no appropriate laser medium exists [1–3]. Crystals such as $LiNbO_3$ and KTP have been the most popular choice of nonlinear optical materials for DFG devices. However, such crystals exhibit large material absorption above 5 μm [4], which limits their operating range for infrared generation.

Mainstream compound semiconductors, particularly AlGaAs, offer significant advantages for infrared generation using optical frequency mixing. AlGaAs benefits from an extended transparency window, covering the spectral range of 0.9–17 μm, high second-order nonlinearity, well-established fabrication technology, and the potential for possible integration with active elements, such as diode lasers. Nevertheless, lack of natural birefringence in AlGaAs makes the phase-matching (PM) $\chi^{(2)}$ processes challenging. To date, several techniques have been successfully reported for PM of DFG processes in AlGaAs, such as form-birefringence phase-matching (BPM) [5,6] and quasi-phase-matching [7,8]. Among these, BPM has been shown to be the most efficient technique. However, the necessity of incorporating AlO_x layers with high absorption above 7.5 μm, along with the absorption of GaAs below 870 nm in wavelength, limits the operating window of BPM devices for infrared generation [1].

Another promising PM technique makes use of Bragg reflection waveguides (BRWs) [9], which rely on utilizing the modal dispersion of one-dimensional photonic bandgap structures. BRW PM has been previously utilized in efficient second-harmonic generation (SHG) [10] and sum-frequency generation [11]. In this Letter, we report Type II DFG in AlGaAs BRWs. The results discussed here are attractive for the implementation of monolithic integrated parametric devices, such as self-pumped DFG devices and integrated photon-pair sources, where a nonlinear element for optical frequency mixing and a diode laser pump are fabricated on the same chip.

The DFG process involves the interaction of a pump at wavelength λ_p, a signal at λ_s, and a difference-frequency (DF) at λ_{DF}. Conservation of energy requires that $\omega_{\mathrm{DF}} = \omega_p - \omega_s$. For maximizing power transfer among the interacting frequencies, the PM condition should be satisfied: $n_{\mathrm{DF}}/\lambda_{\mathrm{DF}} = n_p/\lambda_p - n_s/\lambda_s$, where n_p, n_s, and n_{DF} are the associated mode indices of the pump, signal, and DF, respectively. Using BRW PM, the pump propagates as a Bragg mode, while the signal and DF propagate as total internal reflection (TIR) modes.

A detailed description of the epitaxial structure can be found in [10]. The device characterized here was a ridge waveguide with a ridge width of 4.4 μm and an etch depth of 3.6 μm. The length of the sample was 1.5 mm. The propagation losses of signal and DF around 1550 nm were measured as 2.0 cm^{-1} and 2.2 cm^{-1} for TE and TM polarizations, respectively. The propagation loss of the pump could not be measured directly, owing to the complexities involved in preferentially coupling into the Bragg mode, where a TIR mode also coexists. From a separate SHG experiment [10], an upper value for the loss of the TE Bragg mode around 778 nm was extracted to be 46 cm^{-1}.

Device characterization was carried out in an end-fire coupling setup, which is schematically shown in Fig. 1. A 2 ps mode-locked Ti:sapphire laser operating at 778 nm with a repetition rate of 76 MHz was used as the pump source. The signal was taken from a tunable continuous-wave (CW) C-band tunable laser amplified by an erbium-doped fiber amplifier (EDFA). A tunable fiber grating filter was cascaded with the EDFA to suppress the amplified spontaneous emission (ASE) of the EDFA below the level of the DF. Tunability of the signal wavelength was limited to the 1532–1572 nm range. The range was imposed by the C-band operation of the EDFA and the fiber grating filter. Absolute measurement of DF power requires separation of signal and idler waves at the waveguide output and use of phase-sensitive detection setup. However, due to the proximity of signal and DF wavelengths, the beams could not be separated spatially either by using dispersion prism or by employing narrow-line spectral filters. A rough estimation of the DF power was obtained by carefully calibrating an optical spectrum analyzer (OSA) and integrating the area underneath the DF spectra recorded by

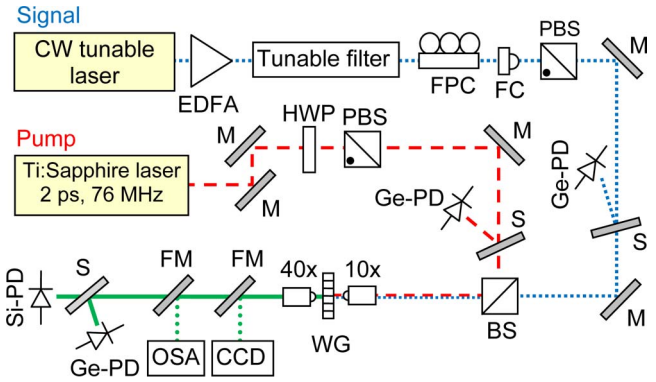

Fig. 1. (Color online) Schematic of the experimental setup: FPC, fiber polarization controller; FC, fiber collimator; HWP, half-wave plate; PBS, polarization beam splitter; BS, beam splitter; S, sampler; M, mirror; WG, waveguide; FM, flip mount; and PD, photodetector.

the OSA, where the error bars were extracted from the measurement variances (12%). We examined Type II DFG, which was about four times more efficient than Type I, where the TE-polarized pump and signal generated TM-polarized DF.

The dependence of the DF power (P_{DF}) on the pump wavelength, for $\lambda_s = 1545.9$ nm, is shown in Fig. 2, where filled circles show the measured data and the solid line is a Lorentzian fit. In obtaining the tuning curve of Fig. 2, the average powers of pump (P_p) and signal (P_s), measured before the front facet of the waveguide, were fixed to 62.9 mW and 2.9 mW, respectively. From the experiment, peak DF power of 0.95 nW, estimated right after the output facet of the waveguide, was obtained for the phase-matched pump at 777.8 nm. The bandwidth of the process was found to be 0.48 nm.

In a DFG process, P_{DF} is proportional to the product of pump and signal powers. We verified this relation for a fixed pump power of 62.9 mW and a signal sweeping power range of 0.48–4.8 mW. The result is shown in the inset of Fig. 2, where the linear fit (dashed line) agrees well with the relation $P_{\mathrm{DF}} \propto P_p P_s$. The slope of the linear fit in the graph of P_{DF} versus $P_p P_s$ provides an estimation of the DFG conversion efficiency defined as $\eta = P_{\mathrm{DF}}/(P_p P_s)$. For the characterized device, η was found to be $\approx 5.7 \times 10^{-4}\%\mathrm{W}^{-1}\ \mathrm{cm}^2$. This efficiency is equal to $2.5 \times 10^{-2}\%\mathrm{W}^{-1}\ \mathrm{cm}^{-2}$ when normalized to the device length.

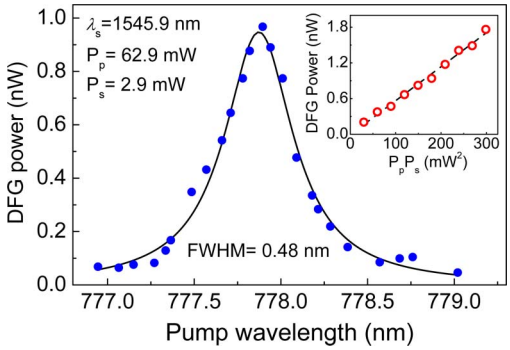

Fig. 2. (Color online) Variation of the DF power as a function of pump wavelength for $\lambda_s = 1545.9$ nm. Filled circles are the measured data and the solid line is the Lorentzian fit. Inset, dependence of P_{DF} on $P_p P_s$. Open circles are the measured data, while the dashed line is a linear fit.

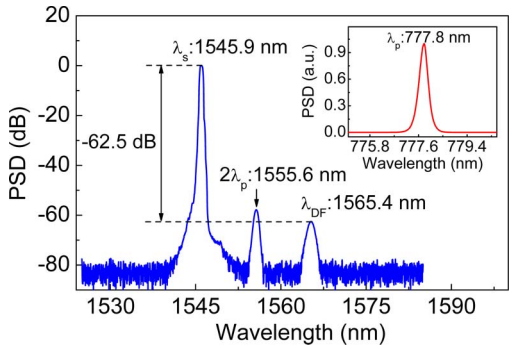

Fig. 3. (Color online) Power spectral density (PSD) of the signal at 1545.9 nm and the converted difference frequency. The central peak at 1555.6 nm is the second-order diffraction of the pump from the OSA internal grating. Inset, pump spectrum.

It should be noted that the DFG efficiency reported here is the external value. The internal efficiency, which requires the estimation of the internal powers inside the device, is considerably larger than the external efficiency. The internal pump power could not be determined due to difficulties in extracting the linear coupling factor—defined as the spatial overlap between the incident pump beam and the excited pump, which is a Bragg mode. Simulations indicate that this coupling efficiency is likely to be a few percent, which implies that a low pump power level is likely to be responsible for the output powers measured. Several routes can be undertaken to further enhance the DFG process in BRWs. These include preferential coupling to the Bragg mode using prism coupling, grating-assisted coupling, or using spatial light modulators. In a more advanced scheme, these coupling techniques can be completely avoided by developing self-pump DFG devices, where a Bragg laser pump [12] with a phase-matched cavity is fabricated on the same wafer platform.

A typical spectrum taken at the waveguide output is shown in Fig. 3. The pump central wavelength was set at 777.8 nm (inset in Fig. 3) with a signal at 1545.9 nm. The DF wavelength was measured to be 1565.4 nm. From the spectra, the power level of DF was –62.5 dB lower than that of the signal. The spectra in Fig. 3 denote an additional spectral feature at $\approx 2\lambda_p = 1555.6$ nm, which is due to the second-order diffraction of the pump from the grating of the OSA. This was confirmed by the fact that the spectral feature at 1555.6 nm remained unchanged,

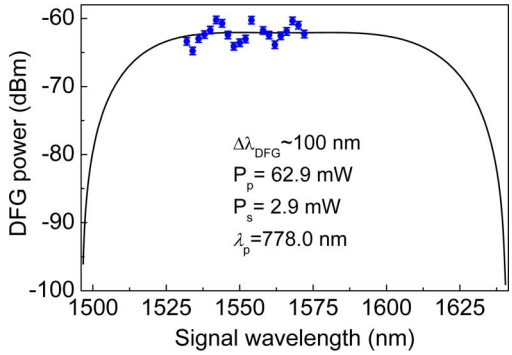

Fig. 4. (Color online) DF power as a function of signal wavelength for the degenerate pump at 778.0 nm. The filled circles are the measured data, and the solid line is the simulated data.

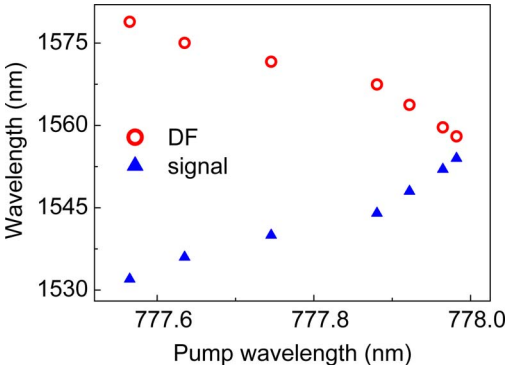

Fig. 5. (Color online) Signal and DF wavelength as a function of pump wavelength.

while the DF spectra shifted in the opposite direction to the signal during tuning.

A key parameter for a DFG device is the PM bandwidth, $\Delta\lambda_{\mathrm{DFG}}$, which determines the useful spectral range within which frequency conversion is efficient. To determine $\Delta\lambda_{\mathrm{DFG}}$, the pump was set at the degenerate wavelength of 778.0 nm, while the generated DF power was monitored and recorded versus signal wavelength in the range of 1532–1572 nm. The result is illustrated in Fig. 4, where the filled circles show the measured data and the solid line is the theoretical curve obtained from numerical simulations. It should be mentioned that the PM peak wavelength obtained from simulation is about 6 nm shorter than that from experiment; the discrepancy is attributed to the uncertainties of the fabrication processes of the device [13]. The spread in the measured power levels, which is denoted by the error bars, was attributed to the cavity resonance effects. The C-band operation of signal laser and the fiber grating filter limited the tunability of the signal beyond the range of 1532–1572 nm. As such, complete measurement of $\Delta\lambda_{\mathrm{DFG}}$ could not be carried out. However, numerical simulations indicated that $\Delta\lambda_{\mathrm{DFG}}$ was approximately 100 nm for this device.

Figure 5 shows the DFG tuning curve, which was obtained by detuning the pump wavelength from degeneracy while tracking the wavelengths of signal and DF for maximal DF power. It was observed that a detuning of the pump wavelength by 0.4 nm resulted in a span of ≈40 nm between signal and DF wavelengths. Further detuning of the pump from degeneracy was expected to offer broader separation between signal and DF. This could not be confirmed experimentally due to the aforementioned constraints in tuning the signal wavelength.

In summary, we reported the first (to our knowledge) demonstration of Type II DFG in AlGaAs BRWs. For a pump power of 62.9 mW and a signal power of 2.9 mW, DF power of 0.95 nW around 1550 nm was observed. The external conversion efficiency was estimated to be $2.5 \times 10^{-2}\%\mathrm{W}^{-1}\ \mathrm{cm}^{-2}$ in a 1.5-mm-long device. The measured DFG showed no sign of bandwidth limitation across a wavelength span of 40 nm, which was limited by instrumentation. The device presented here holds significant promise for the development of monolithic integrated parametric devices.

The authors are thankful to J. S. Aitchison for making the Ti:sapphire laser available and the Natural Sciences and Engineering Research Council of Canada.

References

1. P. Bravetti, A. Fiore, V. Berger, E. Rosencher, J. Nagle, and O. Gauthier-Lafaye, Opt. Lett. **23**, 331 (1998).
2. D. Zheng, L. A. Gordon, Y. S. Wu, R. S. Feigelson, M. M. Fejer, and R. L. Byer, Opt. Lett. **23**, 1010 (1998).
3. K. L. Vodopyanov, Laser & Photon. Rev. **2**, 11 (2008).
4. M. H. Dunn and M. Ebrahimzadeh, Science **286**, 1513 (1999).
5. E. Guillotel, M. Ravaro, F. Ghiglieno, C. Langlois, C. Ricolleau, S. Ducci, I. Favero, and G. Leo, Appl. Phys. Lett. **94**, 171110 (2009).
6. A. Fiore, V. Berger, E. Rosencher, P. Bravetti, N. Laurent, and J. Nagle, Appl. Phys. Lett. **71**, 3622 (1997).
7. S. J. B. Yoo, C. Caneau, R. Bhat, M. A. Koza, A. Rajhel, and N. Anoniades, Appl. Phys. Lett. **68**, 2609 (1996).
8. D. S. Hum and M. M. Fejer, C. R. Physique **8**, 180 (2007).
9. B. Bijlani, P. Abolghasem, and A. S. Helmy, Appl. Phys. Lett. **92**, 101124 (2008).
10. P. Abolghasem, J. Han, A. Arjmand, B. J. Bijlani, and A. S. Helmy, IEEE Photon. Technol. Lett. **21**, 1462 (2009).
11. J. Han, P. Abolghasem, B. J. Bijlani, and A. S. Helmy, Opt. Lett. **34**, 3656 (2009).
12. B. J. Bijlani and A. S. Helmy, Opt. Lett. **34**, 3734 (2009).
13. P. Abolghasem, J. Han, B. J. Bijlani, A. Arjmand, and A. S. Helmy, Opt. Express **17**, 9460 (2009).